Two thermoeconomic diagnosis methods applied to operating data of a commercial refrigeration plant

Torben Ommen, Oskar Sigthorsson, Brian Elmegaard

In order to investigate options for improving the maintenance protocol of commercial refrigeration plants, two thermoeconomic diagnosis methods are evaluated on a state-of-the-art refrigeration plant. A common relative indicator is proposed for the two methods in order to directly compare the quality of malfunction identification. Both methods are applicable to evaluate whether a malfunction in a component corresponds to an intrinsic or an induced malfunction, when using steady state data without measurement uncertainties. By introduction of measurement uncertainty, the identification of intrinsic and induced malfunctions is increasingly difficult. Two different scenarios of measurement uncertainties are evaluated, as the use of repeated measurements yields a lower magnitude of uncertainty. The two methods show similar performance in the presented study for both of the considered measurement uncertainty scenarios. However, only in the lower measurement uncertainty scenario, both methods are applicable to locate the causes of the malfunctions. For both the scenarios a threshold value has been determined for the common relative indicator, which outlines if it is possible to reject a high relative indicator based on measurement uncertainty. Additionally, the contribution of different measuring instruments to relative indicator in two central components is analysed, which shows that the contribution is component dependent.

Nomenclature

$\dot{E}$ exergy rate, [kW]

k unit exergy consumption, [/]

$\dot{m}$ mass flow, [kg/s]

I indicator, [kW]

p pressure, [bar]

$\dot{Q}$ heat rate, [kW]

t temperature, [°C]

UA overall conductance in heat exchanger [kW/K]

$\dot{W}$ power, [kW]

Greek symbols

Δ variation from reference state

δ derivative

ε exergetic efficiency

λ derivative of unit exergy consumption with respect to exergy fuel of a physical component

τ independent thermodynamic variable

Subscripts and superscripts

1-11 state point

add additional operating condition

calc calculated

CT chilled temperature evaporator units

D destruction

F fuel

FT freezing temperature evaporator units

GC gas cooler unit

HP high pressure compressor unit
i component index
k variable index
LP low pressure compressor unit
P product
rel relative to exergy destruction rate in reference operating condition
ref reference operating condition
real real operating condition

1. Introduction

In terms of electricity consumption, the refrigeration sector is a large consumer in many European countries, and even small improvements in the average performance may prove highly beneficial in order to reduce electricity consumption, the dependency of fossil fuels and the environmental concerns. With the maintenance protocol used today, where operation anomalies are often detected and located at set service intervals, malfunctioning components can remain in use for very long periods of time. If a more comprehensive method was used for detecting and diagnosing malfunctions significant energy savings and cost reduction would be possible.

The primary objectives of the thermoeconomic diagnosis approaches are to detect and identify malfunctions on a component level, and to quantify the effects of the system degradation. In general the considered malfunctions are due to operation anomalies, which cause a decreased efficiency of the system, and thus more resources are required in order to obtain the same product.

Malfunctions can be categorised into external, intrinsic and induced malfunctions. The intrinsic malfunctions are the actual causes of malfunctions. The external malfunctions are due to altered conditions outside the system boundary and do not represent degraded components. Together the intrinsic and external malfunctions may induce malfunctions in other components, as the operation conditions may no longer correspond to the expected design or off-design operating condition. Although apparently malfunctioning, components subject to induced malfunctions are not subject to operation anomalies. Using traditional diagnosis methods, the indication of all three types of malfunctions are typically similar. Therefore, to locate the actual causes of malfunctions is a difficult task, as an operation anomaly in one component also affects other components in the system.

In the present study, the thermoeconomic diagnosis approach has been proposed as a method to identify malfunctions on a component level, thus allowing the operator to determine options of corrective actions. The objective of this is to lower the operation time of components with operation anomalies. Thermoeconomic diagnosis can assist in reducing the delay between the start of the operation anomaly and its realisation by the operator of the system. With efficient replacement or repair of the degraded component (once the operation anomaly is detected and located), the malfunctioning components experience reduced operation time with a lowered efficiency, thus reducing the overall electricity consumption. Another benefit of efficient maintenance is the possibility of meeting the full dimensioned capacity at all times, thereby either improving the

security of supply of cold production or allowing for a corresponding down-scale of the refrigeration plant.

Publications based on several different diagnosis approaches have increased in the refrigeration community within the last couple of years [1-4]. Thermoeconomic diagnosis approaches have until recently mainly been proposed and applied to large and complex thermal systems [5]. The focus of the study at hand is to evaluate if the thermoeconomic diagnosis approach for thermal systems may prove useful in smaller applications and at temperatures closer to ambient. The considered system is a small commercial refrigeration plant.

Two previously presented methods to locate the causes of malfunctions are of particular interest. The two methods are:

Method A: Characteristic curves method [6].

Method B: Thermoeconomic models diagnosis approach [7,8].

Both methods have been introduced and used in the TADEUS test case [9,10], which is a steady state combined cycle power plant model. The diagnosis is based on numerical simulations of both design and off-design conditions. In [11] the two methods are compared in terms of usability to locate the causes of malfunctions. The effect of measured data on the thermoeconomic diagnosis approach is considered by Verda et al. [12]. This is done by evaluating the uncertainty of measured data, and later to include the derived uncertainty of measurements in the diagnosis. The evaluation of uncertainties is considered in steady state conditions. In a paper by Usón et al. the operation of a power plant is presented using thermoeconomic diagnosis for a period of more than six years [13].

The objective of this paper is to evaluate the applicability of the two thermoeconomic diagnosis methods to locate the causes of malfunctions in a commercial refrigeration plant for a supermarket, based on a steady state thermodynamic model of the plant, even when measurement uncertainty of practical measurement data is included. A focus of the study is also to evaluate whether the use of the already existing measuring instruments in the system is applicable for further work, or if some of the measuring instruments should be changed or located elsewhere.

2. Methods

Both of the considered methods require operating conditions in a number of different operating points in order to evaluate the behaviour of the components. The component behaviour is used to create models, i.e. in terms of the characteristic curves and the thermoeconomic models for the methods under consideration. The models should be developed prior to the actual diagnosis evaluation. The relations are based on thermodynamic quantities, either from measured data or from a numerical model. A calculation procedure for the application of the two thermoeconomic diagnosis methods using measured data is presented in Figure 1 (A), considering the case where the behaviour of the components has already been modelled. Two calculations are required in order to perform the diagnosis: determination of exergy flows and the actual thermoeconomic diagnosis calculation.

In order to resemble an actual plant with a numerical model, two additional numerical operations are required: evaluation of the thermodynamic quantities based on a numerical model and introduction of measurement uncertainties to the thermodynamic quantities. A graphical representation is included in Figure 1 (B). The numerical operations are:

- A model is developed in order to obtain steady state thermodynamic quantities (T, p, $\dot{m}$) (and electricity consumption, as discussed later) of the refrigeration system without measurement uncertainties.
- Measurement uncertainty is added to the measured thermodynamic quantities.
- A model is required to calculate the exergy flows of the individual streams based only on the measured thermodynamic quantities in the actual plant.
- The two investigated thermoeconomic diagnosis methods are applied individually for the considered components.

The individual parts of the calculation procedure are further discussed in the following subsections. Information on the measurement uncertainty is presented in section 3.2

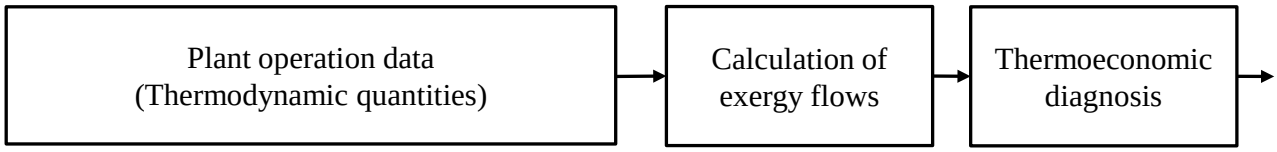

(A)

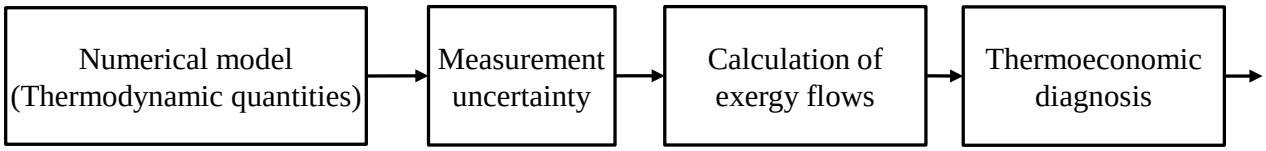

(B)

Figure 1 (A): Procedure to perform diagnosis based on measured data. (B): Procedure to perform diagnosis based on thermodynamic quantities from numerical model with added measurement uncertainty

In order to derive the linearized models, which describe the behaviour of the components, measured thermodynamic quantities are used. Thus yet another level, with the corresponding measurement uncertainties, must be added to the calculation procedure. A schematic illustration of the complete calculation procedure is presented in Figure 2. As an alternative, the approximations could be derived from data directly from a numerical model, in which case the required detail of the model would be subject to further investigation. Furthermore, in this case the approximations of behaviour of the components would not be affected by measurement uncertainty, but subject to any inconsistency between the numerical model and the actual plant operation.

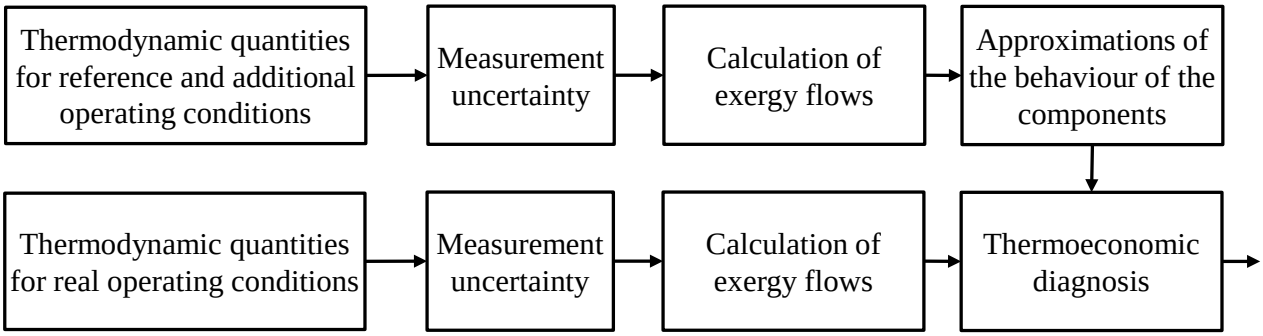

Figure 2: Full calculation procedure to evaluate the impact of measurement uncertainty on the indication of malfunctions in refrigeration plant.

2.1 Numerical model

The conceptual design of commercial refrigeration plants for a supermarket is different from country to country mainly due to differences in legislation and climate. In Denmark, most newly built refrigeration plants are designed much like the one previously presented in literature [3,14]. The refrigerant is Carbon Dioxide (R744). The refrigerant is chosen among different reasons as it is a natural refrigerant with low Global Warming Potential (GWP). A schematic representation of the system including state points is shown in Figure 3.

The acronyms used in Figure 3 represent the main components in the refrigeration cycle: one High Pressure compressor unit (HP), one Low Pressure compressor unit (LP), a Gas Cooler unit (GC), several Chilled Temperature evaporator units (CT) and several Freezing Temperature evaporator units (FT).

The system is scalable to meet refrigeration demands of both large and small commercial applications. In smaller supermarkets the system is usually configured as presented in Figure 3, with two compressors for each stage. The two compressors for each stage are dimensioned for different flow rates. Depending on investment cost, electricity prices and impact on durability, frequency converters are applicable on both compressor stages [15]. The GC fan is operated in order to minimise electricity consumption.

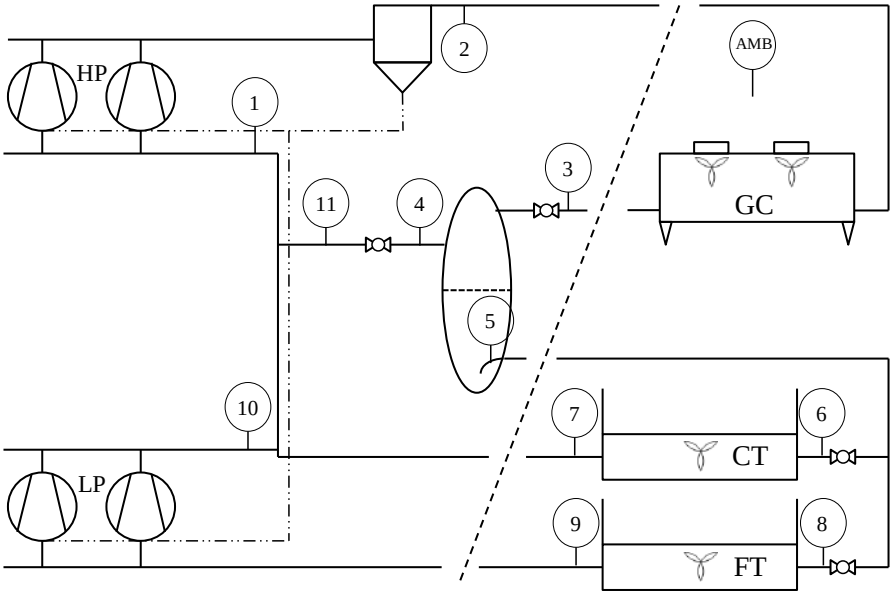

Fig 3: Transcritical refrigeration plant with state points.

In order to evaluate the use of thermoeconomic diagnosis in refrigeration, a numerical model of a transcritical booster refrigeration plant has been implemented. The model is presented in [3]. The purpose of the model is to supply the data needed to substitute measured data from the refrigeration plant. Temperature, pressure and mass flow of each state point are calculated. The use of a numerical model proposes transparency for the reader, easy repeatability and the possibility to obtain steady state thermodynamic data.

Minor revisions have been implemented in the model, compared to the previously published one. The intention of these revisions is to more closely represent the temperature, pressure and mass flow of the actual plant. The parameters of the model are presented in Table 1. The use of coherent state variables between the numerical model and the measurements ensures coherency between the exergy flows in the individual state points and the measurement uncertainties.

The temperature of the refrigerant leaving the GC is closely linked to the operation of the combined refrigeration plant. The use of available experimental data for the numerical model has resulted in a discretised heat exchanger model of the GC. The UA value presented in Table 1 represents the total heat transfer area of the discretised model.

Table 1. Estimated thermodynamic parameters used in the numerical refrigeration plant model.

Parameter	Value	Unit	Description
η_{HP}	0.7	/	HP isentropic efficiency (incl. η_{el})
$\dot{Q}_{HP}$	0	kW	HP heat loss to oil separator and pipes
η_{LP}	0.7	/	LP isentropic efficiency (incl. η_{el})
$\dot{Q}_{LP}$	0	kW	LP heat loss to oil separator and pipes
t_{GC}	32	°C	Temperature of air entering the Gas Cooler
UA_{GC}	8.1	kW/K	Overall conductance in Gas Cooler (sum of discretised model)
p_{GC}	0	kPa	Pressure loss in Gas Cooler
$\dot{W}_{GC,\,fan}$	1.52	kW	Rated fan power in Gas Cooler
$\dot{m}_{GC,\,fan}$	4.72	kg/s	Mass flow of air in Gas Cooler at rated power
$p_{3\text{-}4\text{-}5}$	3500	kPa	Intermediate pressure in liquid receiver
$\dot{Q}_{CT}$	24	kW	Refrigeration load of combined store at CT temperature
UA_{CT}	2.7	kW/K	Conductance in CT evaporator
$t_{SH,CT}$	10	K	Superheat of refrigerant in CT
p_{CT}	0	kPa	Pressure loss in CT
$\dot{W}_{CT,\,fan}$	1	kW	Rated fan power in CT
$t_{CT,in}$	-5	°C	Temperature of air after CT evaporator
$t_{CT,out}$	3	°C	Temperature of air prior to CT evaporator
$\dot{Q}_{FT}$	15	kW	Refrigeration load of combined store at FT temperature
UA_{FT}	0.7	kW/K	Conductance in FT evaporator
$t_{SH,FT}$	10	K	Superheat of refrigerant in FT
p_{FT}	0	kPa	Pressure loss in FT
$\dot{W}_{FT,\,fan}$	1	kW	Rated fan power in FT
$t_{FT,in}$	-25	°C	Temperature of air after FT evaporator
$t_{FT,out}$	-18	°C	Temperature of air prior to FT evaporator

2.2 Calculation of exergy flows

Besides the safety requirements outlined by local legislation, the refrigeration plant is equipped with several temperature indicators and pressure gauges, used for commissioning, regulation and maintenance of the system. The use of already installed measuring instruments is beneficial, as promising results may be directly implemented in supermarkets, where equivalent dimensioning and structure was used, or will be used, during commissioning.

To accommodate the above consideration, a separate model was implemented to evaluate the exergy flow of each stream based the on thermodynamic quantities from the schematics of the refrigeration system, with the measured variables presented in Figure 4. Only measured quantities are allowed as input to the model because this resembles the way experimental data would be used in the thermoeconomic diagnosis. In the evaluation of the exergy flows only the physical constituent is considered, as the chemical composition of the individual streams is assumed constant.

The model was built in EES [16] and is primarily based on energy and mass balances at component level, along with simple assumptions of the refrigerant quality in the evaporators and the receiver.

The thermodynamic quantities (TI and PI – Temperature and Pressure Instrumentation) are used as input parameters. Instrumentations for the mass flows (FI – Flow Instrumentation) of refrigerant

through the compressors are typically not available in newly commissioned plants. The use of flow instrumentation such as coriolis flow meters or similar is possible, or alternatively the refrigerant flow of can be calculated by the assumption of constant rotational speed with fixed electricity frequency. The electricity consumption is monitored for both compressor racks (EI – Electrical Instrumentation). Additional variables are measured for the different evaporators, but due to the investigation detail at component level, further instrumentation is not needed.

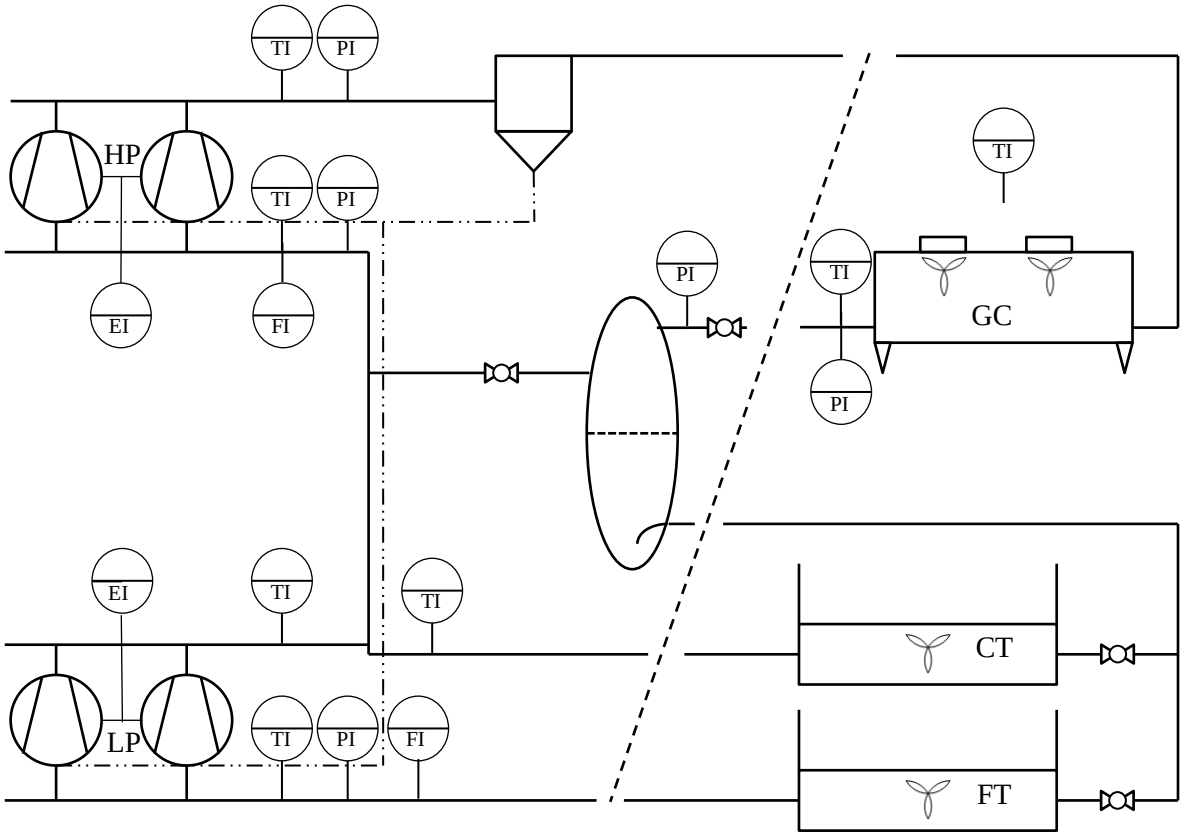

Fig 4: Schematics of the refrigeration system with measured variables. TI – temperature; PI – pressure; FI – Flow; EI – electrical consumption.

Details regarding the instrumentation used for the system and the derived measurement uncertainties are considered in section 3.2.

2.3 Thermoeconomic diagnosis methods

In the study at hand, exergy and exergoeconomic analysis as presented by Bejan et al. [17] is used as the basis of the diagnosis methods. This implies some minor cosmetic changes in the formulation of the two methods, which are presented in this section. Additionally, to achieve a more convenient comparison of the two methods, the derivations of a common relative indicator is presented below.

The characteristic curve method and the thermoeconomic models diagnosis approach have been proposed and discussed in several papers. The definitions used in this work rely solely on the formulation in reference [6] and [12], respectively. In a previously published paper [3], the

characteristic curve method has already been introduced, and applied to the refrigeration plant under consideration, and thus only the thermoeconomic models diagnosis approach is introduced below.

2.3.1 Thermoeconomic models diagnosis approach

The thermoeconomic models diagnosis approach relies on a productive structure, expressed in terms of exergy flows, to describe the physical structure. As an alternative to the productive structure used by Verda et al. [12], the definitions introduced by Bejan et al. [17] can be used.

The identification between the intrinsic and induced malfunction is accomplished with a comparison between the real and reference operating conditions. This is done by describing the behaviour of the component using the unit exergy consumption (the ratio between the exergy fuel and product rates, i.e. for the *ith* component as $k^i = \dot{E_F}^i / \dot{E}_P^i$) as the dependent variable and the exergy fuel rate as the independent variable. To compare the two operating conditions, the expected exergy product rate at the reference operating condition is calculated. An approach was used to linearly approximate the exergy product rate from the real operating condition back to the reference operating condition. This is expressed for the *ith* component as:

$$\dot{E}_{P,ref}^{i,calc} = \dot{E}_{P,real}^{i} + \lambda^i (\dot{E}_{F,ref}^{i} - \dot{E}_{F,real}^{i}),$$

where the subscripts *ref* and *real* refer to the reference and real operating conditions, respectively. Furthermore, λ^i refers to the derivative of the unit exergy consumption with respect exergy fuel rate at the reference operating condition, i.e. $\lambda^i = \left[\partial k^{i,ref} / \partial \dot{E}_F^i \right]_{E_F^{i,ref}}$.

In the formulation of the productive structure used by Verda et al. the level of detail of the productive structure can be increased by splitting the exergy flows into thermal and mechanical components. However, limited improvement in the accuracy of the thermoeconomic diagnosis is gained [18]. In cases where the exergy fuel consists of two or more physical streams, the expected exergy product rate is based on linearization of each individual physical stream, rather than only one fuel/product relationship. This approach has been adopted in order to resemble the formulation used in [12]. Therefore, considering a case where two physical streams are supplied to a component, the expected exergy product rate is expressed for the *ith* component as:

$$\dot{E}_{P,ref}^{i,calc} = \dot{E}_{P,real}^{i} + \lambda_1^i (\dot{E}_{F1,ref}^{i} - \dot{E}_{F1,real}^{i}) + \lambda_2^i (\dot{E}_{F2,ref}^{i} - \dot{E}_{F2,real}^{i}).$$

To develop the derivatives, additional operating condition, which are equal in number to the degrees of freedom, in the vicinity of the reference operating condition are required. Since the degrees of freedom are decreased to one by the productive structure, except for the cases where two or more physical streams are supplied to the component (where the degrees of freedom are equal to number of physical streams), only one additional operating condition is needed. The additional operating conditions are obtained by varying the operating conditions near the reference operating condition, by varying the ambient conditions or the plant load. For the *ith* component, and considering a case where two physical streams are supplied to a component, the approximation of the derivatives is accomplished by solving the following system of equations for the derivatives λ_1^i and λ_2^i:

$$\dot{E}^i_{P,ref} = \dot{E}^{\,i}_{P,add1} + \lambda^i_1\left(\dot{E}^i_{F1,ref} - \dot{E}^i_{F1,add1}\right) + \lambda^i_2(\dot{E}^i_{F2,ref} - \dot{E}^i_{F2,add1}),$$
$$\dot{E}^i_{P,ref} = \dot{E}^{\,i}_{P,add2} + \lambda^i_1\left(\dot{E}^i_{F1,ref} - \dot{E}^i_{F1,add2}\right) + \lambda^i_2(\dot{E}^i_{F2,ref} - \dot{E}^i_{F2,add2}),$$

where the subscript *add* refers to the additional operating condition.

2.3.2 Common indicator

The proposed indicator compares the real and reference operating conditions. More precisely, for the thermoeconomic models diagnosis approach, it indicates the difference between the exergy product rate and the expected exergy product rate at the reference operating condition. If the expected exergy product rate is lower than the exergy product rate, increased exergy destruction rate occurs in the component, and the difference is caused by an intrinsic malfunction. The indicator is formulated for the *ith* component as:

$$I^i = \Delta\dot{E}^i_D - \Delta\dot{E}^{i,calc}_D = \dot{E}^i_{P,ref} - \dot{E}^{i,calc}_{P,ref}. \quad (3)$$

The defined indicator depends on the absolute exergy destruction rate in the component. In an evaluation of a complete plant operation, the use of a relative indicator might assist in locating the crucial degraded component. The proposed relative indicator is defined for the *ith* component using the exergy destruction rate at the reference operating condition:

$$I^i_{rel} = \mathrm{I}^{\mathrm{i}}/\dot{E}^i_{D,ref} = (\dot{E}^i_{P,ref} - \dot{E}^{i,calc}_{P,ref})/\dot{E}^i_{D,ref} \quad (4)$$

Identically, the relative indicator for the characteristic curve method used in Ommen et al. [3] can be revised to match the relative indicator defined in Equation 4:

$$I^i_{rel} = \mathrm{I}^{\mathrm{i}}/\dot{E}^i_{D,ref} = (\Delta\dot{E}^i_D - \Delta\dot{E}^i_{D,calc})/\dot{E}^i_{D,ref} \quad (5)$$

3. Results

A calculation example is carried out throughout the paper. Beside the reference and additional operating conditions, four operating conditions with malfunctions are considered, denoted as:

Real 1: Increased operation pressure in refrigerant receiver by 300 kPa.

Real 2: Reduction in LP-compressor isentropic efficiency by 0.1 /.

Real 3: Reduction in HP-compressor isentropic efficiency by 0.1 /.

Real 4: Malfunctioning fan at air side of the Gas Cooler -> mass flow of air reduced by 50%.

Malfunctions are evaluated for the five main components of the refrigeration plant. The five components are marked with acronyms in Figure 3. The three latter operating conditions include an intrinsic malfunction in one of the components under consideration. However, the first operating condition only includes induced malfunctions in the components under consideration. No external malfunctions are included in the respective operating conditions.

The reference and real operating conditions of the refrigeration plant, according to the state points defined in Figure 3, are presented in the appendix.

3.1 Evaluation of the thermoeconomic diagnosis methods without measurement uncertainties

The initial evaluation is carried out using steady state data obtained from the numerical model of the refrigeration plant, without measurement uncertainties. With regards to Figure 1 (B), the procedure is performed without measurement uncertainties.

The obtained results are presented in Tables 2 – 3 for both of the considered thermoeconomic diagnosis methods. For both methods, some of the sub results are included, as this allows for a convenient comparison with the referenced papers [6,12]. In the sub-table to the right of Tables 2 and 3, the proposed common relative indicator is presented, with highlighted colour in the areas where intrinsic malfunctions should be present according to the respective operation anomalies.

Table 2: Calculation example of method A

	$\dot{E}^i_{D,real}$ [kW]				$\Delta\dot{E}^i_D$ [kW]				$\Delta\dot{E}^i_{D,calc}$ [kW]				I^i_{rel} [/]			
	Real 1	**Real 2**	**Real 3**	**Real 4**	**Real 1**	**Real 2**	**Real 3**	**Real 4**	**Real 1**	**Real 2**	**Real 3**	**Real 4**	**Real 1**	**Real 2**	**Real 3**	**Real 4**
HP Comp	3.60	3.60	5.51	3.76	0.01	0.01	1.93	0.18	0.01	0.01	0.32	0.18	-0.1	0.0	44.6	-0.4
GC HEX	5.51	5.57	6.16	5.93	0.00	0.05	0.65	0.41	0.00	0.07	0.78	4.74	0.1	0.2	1.6	43.5
MT HEX	0.89	0.90	0.90	0.89	0.00	0.00	0.00	0.00	0.01	0.00	0.00	0.00	-1.1	0.0	0.0	0.0
LT HEX	0.24	0.24	0.24	0.25	0.00	0.00	0.00	0.00	0.00	0.00	0.00	0.00	-1.0	0.0	0.0	0.0
LP Comp	0.28	0.42	0.27	0.27	0.01	0.15	0.00	0.00	0.01	0.03	0.00	0.00	0.7	43.5	0.0	0.0

Table 3: Calculation example of method B

	$\dot{E}^i_{P,real}$ [kW]				$\dot{E}^{i,calc}_{P,ref}$ [kW]				$\dot{E}^i_{P,ref} - \dot{E}^{i,calc}_{P,ref}$ [kW]				I^i_{rel}[/]			
	Real 1	**Real 2**	**Real 3**	**Real 4**	**Real 1**	**Real 2**	**Real 3**	**Real 4**	**Real 1**	**Real 2**	**Real 3**	**Real 4**	**Real 1**	**Real 2**	**Real 3**	**Real 4**
HP Comp	45.3	45.3	45.9	46.8	45.2	45.2	43.7	45.2	0.00	0.00	1.48	-0.01	0.0	-0.1	41.3	-0.4
GC HEX	39.9	39.7	39.7	40.9	39.7	39.7	39.7	41.7	-0.00	0.00	0.00	2.04	0.0	0.0	0.0	37.0
MT HEX	16.8	16.4	16.4	16.4	16.3	16.4	16.4	16.4	0.04	0.00	0.00	0.00	1.5	0.0	0.0	0.0
LT HEX	3.5	3.4	3.4	3.4	3.4	3.4	3.4	3.4	0.01	0.00	0.00	0.00	0.9	0.0	0.0	0.0
LP Comp.	4.2	4.1	4.1	4.1	4.1	4.0	4.1	4.1	0.00	0.11	0.00	0.00	1.6	40.2	0.0	0.0

The results show that both diagnosis methods can identify the intrinsic malfunctions and filter out induced malfunctions that are due to the changed operating point, caused by intrinsic malfunctions in other components. From the small relative indicators for components with induced malfunctions it seems plausible, that the use of linearized models of the behaviour of the components is sufficient to identify the operation anomalies.

The relative indicators of components with intrinsic malfunctions in the different malfunctioning operating conditions are of equal magnitude between the two methods considered. The differences

in the relative indicators for components with induced malfunctions (especially in Real 1) are slightly increased for method B. The two methods are considered equally demanding in terms of their calculation procedures and evaluation time.

3.2 Evaluation of the thermoeconomic diagnosis methods with measurement uncertainties

In order to include measurement uncertainty in the system, the thermoeconomic diagnosis procedure must be repeated with the new information. The plant data presented in the appendix is still applicable, but with added uncertainty as presented in Figure 1 (B). Assumptions for the measuring instruments are presented in Table 4. Furthermore, the impact of the measurement uncertainty is evaluated based on the previously presented results from Table 2 and 3.

It is assumed, that when thermoeconomic diagnosis is applied on the refrigeration plant, both the reference and additional operating conditions to approximate the characteristic curves and the thermoeconomic models, will be based on data with measurement uncertainty. Therefore, the approximated behaviour of the components includes measurement uncertainty from the corresponding measuring instruments. As the measurement of the thermodynamic quantities used for the evaluation is done by the same instruments repeatedly, special conditions apply, which are considered below.

Table 4 presents the measurement uncertainty of the evaluated measuring instruments in two scenarios, denoted as worst case and estimated scenarios. The worst case scenario represents the full measurement uncertainty of the instrument used in the study. The worst case data is based on information from the instrument datasheets [19-21]. The measurement uncertainties of the FI instruments are based on estimations. However, as the measurement uncertainty from the FI instruments is important for the study at hand, the effect of the considered measurement uncertainty is further investigated in section 3.3. The measurement uncertainty used for FI instruments in both of the cases considered in Table 4 is significantly higher than what is possible when using coriolis flow meters [22].

Table 4: Measurement uncertainty of the evaluated measuring instruments in the two scenarios

			Deviation (k=2)		
Measured quantity	State points	Full Scale / Relative	Worst case	Estimated	Unit
Temperature	All	Full scale	0.5	0.1	C
Pressure	2; 3	Full scale	128	16	kPa
	1; 4; 15	Full scale	48	6	kPa
Mass flow of refrigerant	1; 15	Relative	2	1	%
Electricity consumption	1; 15	Relative	1.2	0.6	%

The use of the worst case measurement uncertainty scenario does not take into consideration that uncertainty of measurement is composed into several different components related to the actual measuring instrument, of which typically only a minor part of the uncertainty is measuring hysteresis and repeatability. Thus only a part of the measurement uncertainty is likely represented

correctly by the estimated case. For several of the instrumentation types used in the investigation, the individual uncertainty components, such as the contribution of hysteresis, are listed in the datasheets [20,22]. In the case where the approximations of the characteristic curves and the thermoeconomic models of the components are based on measured thermodynamic quantities, the approximations will correspondingly include the offset, such as linearity deviation and thermal zero point from the calibration of its measuring instruments [20].

As for the measurement uncertainties assumed in Table 4, the resulting uncertainty on the derived relative indicators has been calculated using *k=2* (results shown with 95% confidence). The effects of measurement uncertainties on the relative indicators calculated in Tables 2 and 3 are presented in Figures 5 – 8.

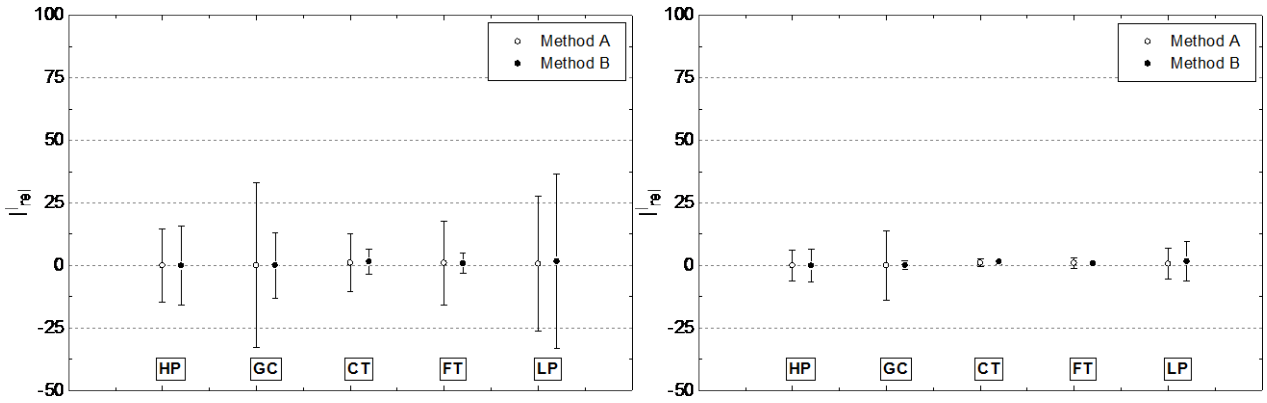

(A) *(B)*

Fig 5: The effect of measurement uncertainties on the proposed relative indicator for Real 1 with two different uncertainty scenarios: (A) Worst Case (B) Estimated.

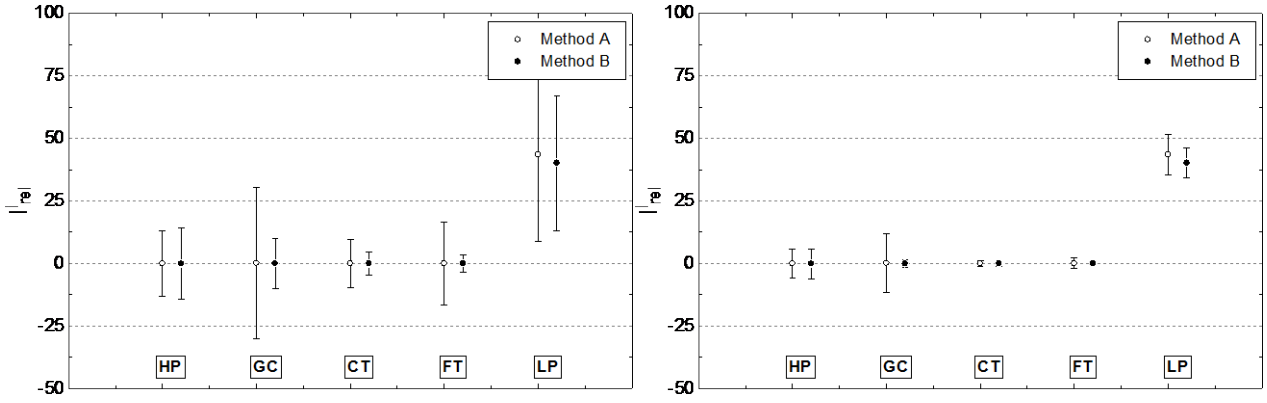

(A) *(B)*

Fig 6: The effect of measurement uncertainties on the proposed relative indicator for Real 2 with two different uncertainty scenarios: (A) Worst Case (B) Estimated.

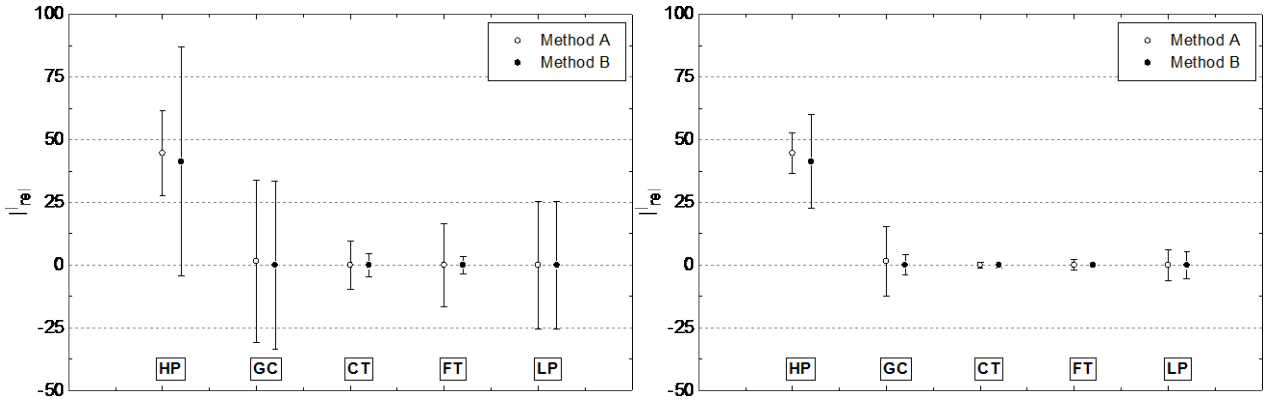

(A) *(B)*

Fig 7: The effect of measurement uncertainties on the proposed relative indicator for Real 3 with two different uncertainty scenarios: (A) Worst Case (B) Estimated.

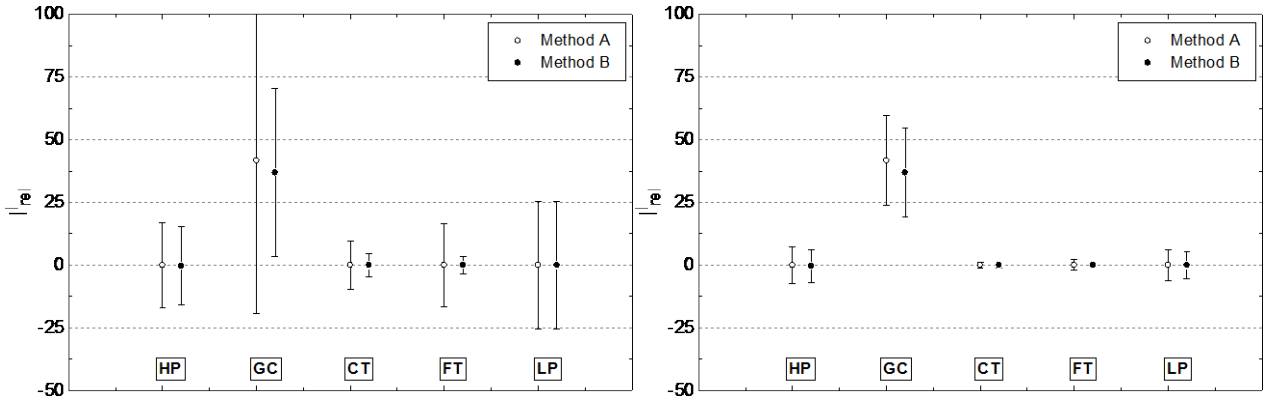

(A) *(B)*

Fig 8: The effect of measurement uncertainties on the proposed relative indicator for Real 4 with two different uncertainty scenarios: (A) Worst Case (B) Estimated.

The Figures 5-8 individually show the effect of measurement uncertainties on the relative indicator for each of the four operating conditions with malfunctions. The results on the left hand side (A) represent the worst case measurement uncertainty scenario, while the results presented on the right hand side (B) represents the estimated uncertainty scenario. In each of the eight sub-figures the results for both diagnosis methods are presented concurrently for each considered component.

Four main deductions can be drawn from Figures 5 – 8:

- Both methods are applicable to locate the causes of malfunctions for the estimated measurement uncertainty scenarios. For method A, a significant margin is present between induced and intrinsic malfunctions in all cases. For method B, the lower value of the relative indicator for the GC leads to a small margin between induced and intrinsic malfunction in the Real 4 operating condition.

- In the worst case scenario, overlaps between the relative indicators for components with intrinsic and induced malfunctions due to measurement uncertainties are present for both methods A and B. The overlaps are typically most dominant using method B.
- The impact of the measurement uncertainty on the relative indicator is of equal magnitude for the two methods, considering both measurement uncertainty scenarios.
- For the worst case uncertainty scenario, a relative indicator above the value of $I_{rel} = 30$ indicates an intrinsic malfunction in the considered components. Using the estimated uncertainty scenario, the threshold value of the relative indicator for induced effects is approximately $I_{rel} = 15$ for the characteristic curves method, and $I_{rel} = 8$ for the thermoeconomic models diagnosis approach.

3.3 Critical measuring instrument

According to the above results, the measurement uncertainty cannot be neglected. An assessment of the individual contributions to the combined uncertainty may thus increase the quality of the diagnosis. The assessment is performed for two components (HP and GC) using the characteristic curves method (method A).

The evaluation is based on a variation of the relative measurement uncertainty from the mass flow measuring instruments between zero and worst case scenario values. The worst case measurement uncertainty scenario is used for temperature and pressure transmitters throughout the evaluation, according to Table 4.

For the HP the contributions of measurement uncertainty from its measuring instruments are presented in Figure 9. The displayed lines represent the collected uncertainty of the specific instrument, e.g., all the employed pressure measurements are contained in one overall contribution. The four inputs to the diagnosis procedure (temperature, pressure, mass flow and electricity consumption) are normalised to present their relative impact on the combined uncertainty. The resulting uncertainty on the relative indicator ±u(I^i_{rel}) is presented on the right hand ordinate axis. The resulting uncertainty corresponds to the uncertainty of the relative indicator used in Fig. 5-8.

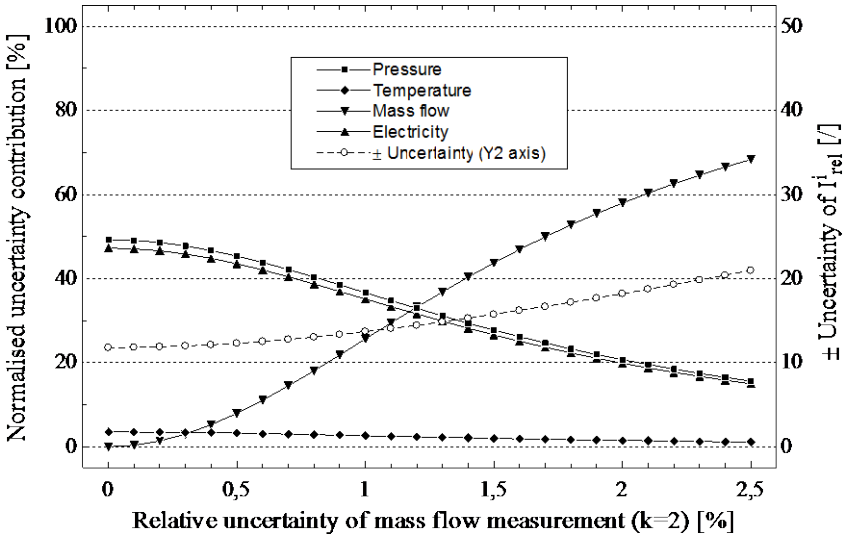

Fig 9: Evaluation of the individual contributions of measurement uncertainties for the HP-compressor. The combined measurement uncertainty on the relative indicator $\pm u(I_{rel}^{i})$ is presented on the second ordinate.

For low measurement uncertainties from the mass flow instrumentation, uncertainty from electricity and pressure measurement instruments are by far the major component in the comparison. With increasing relative measurement uncertainty of mass flow, the contribution of flow measurements is increased above the contribution of pressure measurements. In the considered range, the contribution from flow instrumentation is at maximum 65% of the combined uncertainty.

For the Gas Cooler unit, a similar evaluation of the measurement uncertainty contribution has been performed and is presented in Figure 10. The main contribution of measurement uncertainty is from the various temperature measurements. Even with high relative uncertainty of the mass flow of refrigerant, more than 95% of the uncertainty corresponds to temperature measurement. Figures 9 and 10 show clear differences in trends between the contributions of measurement uncertainty from the individual types of units investigated. The result is presented in Figure 10 and shows very limited variations.

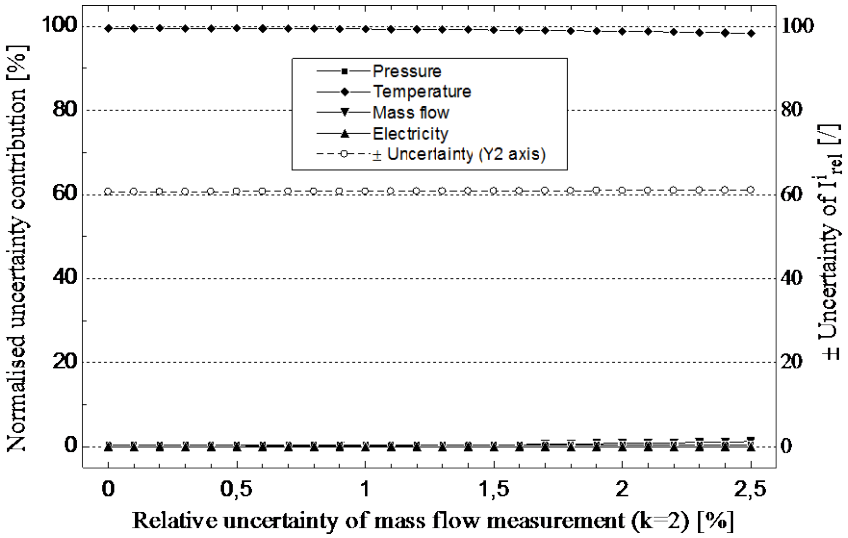

Fig 10: Evaluation of the individual contributions of measurement uncertainties for the Gas Cooler unit. The combined measurement uncertainty on the relative indicator $\pm u(I_{rel}^{i})$ is presented on the second ordinate.

4. Discussion

The objective of the paper has been to evaluate the performance of two thermoeconomic diagnosis methods applied on a refrigeration plant where measurement uncertainty is included in the reference, additional and malfunctioning operating conditions. From the results, it is possible to state an expected confidence in the quality of measured relative indicators in an equivalent commercial refrigeration plant, if the data is obtained from steady state operation. Both thermoeconomic diagnosis methods have proved applicable with the measuring instruments considered in this study using the estimated uncertainty scenario.

It should be noted that achieving the maximum uncertainty in the relative indicator, shown by the uncertainty bars for both scenarios in Figure 5 – 8, is only possible if a number of measurements have experienced their maximal and diverging measurement uncertainty (k=2), in the thermoeconomic diagnosis procedure presented in Figure 2. With the possibility of repeated measurements a lower coverage factor could be used (e.g. k=1).

Based on the analysis of the contribution of each measuring instrument on the measurement uncertainties performed in Figures 9 – 10, it is clear that even a relatively high measurement uncertainty from the flow instrumentation does not contribute significantly to the combined measurement uncertainty or to the quality of the relative indicators. As the worst case measurement uncertainty of mass flow instrumentation is considered as a high value, no further attempt is done to quantify the uncertainty of such instrumentation.

Several other factors may contribute in an actual application of the two thermoeconomic diagnosis methods. Therefore, it is difficult to discuss the impact of highly fluctuating load demand and transient operation, like the one often experienced in a commercial refrigeration plant, especially in poorly designed systems where the compressor capacity does not match the different part-load demands. Such analysis has not yet been addressed in literature with respect to the two diagnosis methods. It is expected that unbalanced systems may interfere additionally to the uncertainty of the relative indicator. Such effects may challenge the applicability of thermoeconomic diagnosis. On the other hand, the diagnosis methods will not require a constant full-time monitoring and analysis to evaluate the components, but can be enabled when operation is performing in steady state, i.e. close to the design load.

If real steady state observations are not possible to achieve, it may as such be possible to construct a numerical filter to bypass unusable information from the collected data, thus only employ quasistatic measurements in the actual diagnosis procedure. This may on the other hand decrease the quality of the measurements.

Two different measurement uncertainty scenarios are evaluated. The use of the estimated scenario represents the case where the approximation of numerical models allows a simple calibration of the measuring instruments at different reference operating conditions. Using this approach, some of the individual measuring uncertainty contributions, as e.g. linearity deviation and thermal zero point, disappear. This is possible if the characteristic curves and the thermoeconomic models are approximated for a specific refrigeration plant using different measured reference and additional operating conditions data.

A significant choice in the application of the two thermoeconomic diagnosis methods is the choice of the additional operating conditions (and the independent and dependent variables in the characteristic curve method) to approximate the behaviour of the components, i.e. in terms of the characteristic curves and the thermoeconomic models for the respective methods under consideration. It is the experience of the authors of this paper, that the selection of the additional operating conditions to accomplish this influences the quality of the diagnosis, although this should intuitively not be the case. Correspondingly it is not certain, that the choice of the additional

operating conditions or variables, at the same time yields a satisfactory indication of malfunctions and also a low measurement uncertainty.

In a case where the approximated characteristic curves and thermoeconomic models of the components in one refrigeration system, are applied on another refrigeration system, the measurement uncertainties can possibly be larger than the ones presented by the worst case measurement uncertainty scenario. This is because the reference operating condition used in the former refrigeration system does not necessarily match the reference operating condition of the second system, as well as the linearity deviation and thermal zero point most likely is changed with a different set of measuring instruments.

5. Conclusion

Two thermoeconomic diagnosis methods have been evaluated in terms of their applicability within commercial refrigeration. A common relative indicator for the two methods is proposed, which can be used to directly compare the quality of the identification of intrinsic and induced malfunctions.

Both methods are applicable to evaluate whether a malfunction is intrinsic or induced when using steady state data without measurement uncertainties. The quality of the results is considered equivalent between the two methods. The data supplied to the diagnosis matches the location of already installed measuring instruments, except for the case of flow instruments.

With the introduction of measurement uncertainties, several approaches are possible. In this study the approximations of component behaviours have been calculated based on measured data, with measurement uncertainty. The study is based on two different measurement uncertainty scenarios from the measuring instruments under consideration. Using the worst case uncertainty scenario, both methods show overlaps between the relative indicators for components with intrinsic and induced malfunctions due to measurement uncertainties. With the estimated scenario, which represents repeated measurements of fixed instrumentation, both methods are applicable to locate the causes of malfunctions with significant margin between induced and intrinsic malfunctions. For the worst case uncertainty scenario, a relative indicator above $I_{rel} = 30$ indicates an intrinsic malfunction in the considered component. Using the estimated uncertainty scenario, the threshold value of the relative indicator for induced effects is $I_{rel} = 15$ for the characteristic curves method, and $I_{rel} = 8$ for the thermoeconomic models diagnosis approach.

The case with the highest measurement uncertainty is used for a brief evaluation of the contribution from different measurement instruments using the characteristic curves method. The evaluation shows that the highest contributor of measurement uncertainty from the measuring instrument is component dependent. In the transcritical (HP) compressor unit the most important is the flow measurement instrument, while for the gas cooler the combined contribution of temperature measurement instruments are the most important.

Acknowledgements

The work was supported by the Danish Energy Technology Development and Demonstration programme (EUDP).

Appendix

The plant data for the reference operating condition and the four operating conditions with malfunctions (Real 1 - 4).

Variable	Unit	REF	Real 1	Real 2	Real 3	Real 4
T_1	K	270.7	270.5	271.3	270.7	270.4
T_2	K	380.6	380.3	381.5	390.6	383.6
T_3	K	305.6	305.6	305.6	305.6	307.0
T_7	K	272.6	272.6	272.6	272.6	272.6
T_9	K	252.8	252.8	252.8	252.8	252.8
T_{10}	K	304.8	304.8	310.8	304.8	304.8
T_{amb}	K	305.1	305.2	305.2	305.2	305.2
p_1	kPa	2607	2607	2607	2607	2607
p_2	kPa	8651	8652	8651	8652	8945
p_3	kPa	8651	8652	8651	8652	8945
p_4	kPa	3500	3800	3500	3500	3500
p_9	kPa	1409	1409	1409	1409	1409
$\dot{m}_{HP}$	kg/s	0.197	0.197	0.197	0.197	0.202
$\dot{m}_{LP}$	kg/s	0.024	0.025	0.024	0.024	0.024
$\dot{W}_{HP}$	kW	15.4	15.5	15.5	18.0	16.3
$\dot{W}_{LP}$	kW	0.94	0.97	1.10	0.94	0.94

References

[1] Green T, Izadi-Zamanabadi R, Niemann H. On the choice of performance assessment criteria and their impact on the overall system performance - The refrigeration system case study. Conf Control Fault-Tolerant Syst , SysTol - Final Program Book Abstr 2010:624-9.

[2] Tassou SA, Grace IN. Fault diagnosis and refrigerant leak detection in vapour compression refrigeration systems. Int J Refrig 2005;28:680-8.

[3] Ommen T, Elmegaard B. Numerical model for thermoeconomic diagnosis in commercial transcritical/subcritical booster refrigeration systems. Energy Convers Manage 2012;60:161-9.

[4] Piacentino A, Talamo M. Critical analysis of conventional thermoeconomic approaches to the diagnosis of multiple faults in air conditioning units: Capabilities, drawbacks and improvement directions. A case study for an air-cooled system with 120 kW capacity. Int J Refrig 2013;36:24-44.

[5] Valero A, Correas L, Lazzaretto A, Rangel V, Reini M, Taccani R et al. Thermoeconomic philosophy applied to the operating analysis and diagnosis of energy utility systems. Int J Thermodyn 2004;7:33-9.

[6] Toffolo A, Lazzaretto A. A new thermoeconomic method for the location of causes of malfunctions in energy systems. J Energy Resour Technol Trans ASME 2007;129:1-9.

[7] Verda V, Serra L, Valero A. Zooming procedure for the thermoeconomic diagnosis of highly complex energy systems. Int J Appl Thermodyn 2002;5:75-83.

[8] Verda V, Serra L, Valero A. A procedure for filtering the induced effects in the thermoeconomic diagnosis of an energy system. ASME Adv Energy Syst Div Publ AES 2001;41:447-55.

[9] Valero A, Correas L, Zaleta A, Lazzaretto A, Verda V, Reini M et al. On the thermoeconomic approach to the diagnosis of energy system malfunctions Part 1: The TADEUS problem. Energy 2004;29:1875-87.

[10] Valero A, Correas L, Zaleta A, Lazzaretto A, Verda V, Reini M et al. On the thermoeconomic approach to the diagnosis of energy system malfunctions Part 2. Malfunction definitions and assessment. Energy 2004;29:1889-907.

[11] Lazzaretto A, Toffolo A, Reini M, Taccani R, Zaleta-Aguilar A, Rangel-Hernandez V et al. Four approaches compared on the TADEUS (thermoeconomic approach to the diagnosis of energy utility systems) test case. Energy 2006;31:1586-613.

[12] Verda V, Borchiellini R. Exergy method for the diagnosis of energy systems using measured data. Energy 2007;32:490-8.

[13] Usón S, Valero A, Correas L. Energy efficiency assessment and improvement in energy intensive systems through thermoeconomic diagnosis of the operation. Appl Energy 2010;87:1989-95.

[14] Ge YT, Tassou SA. Thermodynamic analysis of transcritical CO2 booster refrigeration systems in supermarket. Energy Convers Manage 2011;52:1868-75.

[15] Advansor A/S. compSUPER S. compSUPER, Advansor 2013;Accessed 2013:http://www.advansor.dk/.

[16] F-Chart Software (LLC.). Engineering Equation Solver. EES 1992;V9.710 (6/28/12):http://www.fchart.com/ees/.

[17] Bejan A, Tsatsaronis G, Moran M. Thermal Design & Optimization. 1'st edition ed. New York: John Wiley & Sons, 1996.

[18] Verda V. Accuracy level in thermoeconomic diagnosis of energy systems. Energy 2006;31:3248-60.

[19] Danfoss A/S. Data sheet/ technical leaflet, AKS 11, PT1000 Temperature Sensor, Superheat Measurement.
 . 2012;Accessed 2013:http://www.danfoss.com/.

[20] Danfoss A/S. Data sheet/ technical leaflet, AKS 2050, Pressure Transmitter. 2012;Accessed 2013:http://www.danfoss.com/.

[21] ABB inc. DELTAplus, Technical Documentation, DIN Rail Mounted electricity meters, DBB13000. 2013;Accessed 2013:http://www.abb.com/.

[22] Siemens AG. Coriolis flowmeters, SITRANS F C MASS 2100 Di 3-40. 2013;Accessed 2013:http://www.automation.siemens.com.